Ab initio and density functional study of structure and bonding of cage compounds containing boron, phosphorus and group 14 atoms†

Sofia Pachini and Michael P. Sigalas*

Laboratory of Applied Quantum Chemistry, Department of Chemistry, Aristotle University of Thessaloniki, 54124, Thessaloniki, Greece. E-mail: sigalas@chem.auth.gr; Fax: (+2310) 99 77 38; Tel: (+2310) 99 78 15

Received* (*in Toulouse, France*) *29th January 2003, Accepted 10th April 2003
First published as an Advance Article on the web 2nd July 2003

Ab initio and density functional calculations for five vertex cage compounds of the type $P_2(YB)_2EH_2$, (E = C, Si, Ge, Sn, Y = H, H_2N) using 6-311G++(d,p) and 3-21G++(d,p) basis sets, showed that they adopt a trigonal bipyramidal structure of C_{2v} symmetry with the two phosphorus atoms occupying the apical position, the HB or NB groups residing in the trigonal basal plane. The theoretical results agree well with the experimental data for E = Si, Ge and Sn. For the carbon cage $P_2(HB)_2CH_2$ this structure is a transition state and the minimum is a cage of C_s symmetry with a distorted B–B–C ring in the equatorial plane. Key structural parameters within the cages show a linear dependence on the covalent radii and the diffuseness of the orbitals of the heteroatom E. The results of the natural population analysis (NPA) and the values of nucleus independent chemical shifts (NICS) calculated reveal a bonding description very close to the idealized localized Lewis structure, in contrast to the parent $P_2(HB)_3$ cage. This is more pronounced in the case of the NH_2 substituted cages.

Introduction

Inorganic ring and cage compounds containing boron have attracted much attention over the years due to their fundamentally interesting structural and electronic features, as well as their potential utility as solid state materials precursors.[1–10] In particular, cage compounds containing boron and phosphorus atoms continue to increase and diversify. Recently Nöth and Paine have developed general assembly approaches for $B_xP_yE_z$ cage compounds and a number of five vertex cage compounds of the type $P_2(R_2NB)_2ER_2$, (E = Si, Ge, Sn) have been prepared and structurally characterized.[11–13]

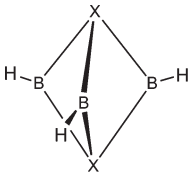

1a X = N, CH, P, SiH, BH^- **1b**

The electronic structures of heterocapped five-vertex species of the type 1,5-$X_2B_3H_3$ (X = N, CH, P, SiH, BH^-) have been discussed many times in the literature.[1,14–26] One of the main goals of these works was the bonding description of these species in terms of either classical, **1a**, or "delocalized" or non-classical, **1b**, electronic representations.

In this work, we describe the results of *ab initio* and density functional calculations for the five vertex cage compounds of the type $P_2(YB)_2EH_2$, where E = C, Si, Ge, Sn and Y = H (**2**) and H_2N (**3**). Although these systems have been systematically

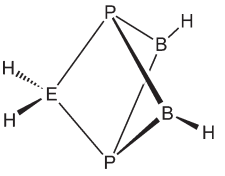

2 E = C, Si, Ge, Sn

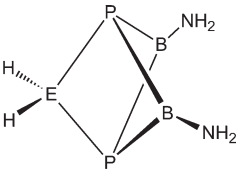

3

studied experimentally,[11–13] there were no theoretical data available. The molecular structures of all cages have been optimized at both levels of theory using the 6-311G++(d,p) and 3-21G++(d,p) basis sets and the variation of geometry as a function of the covalent radii and the diffuseness of the orbitals of the heteroatom E is examined. The nature of bonding, the extent of B–B interaction and the effect of the NH_2 substituents are discussed in the light of the natural population analysis (NPA), whereas the calculated nucleus independent chemical shifts (NICS) were used as a measure of stability across the series.

Computational details

Ab initio calculations were performed at the second-order Møller–Plesset perturbation theory (MP2). For the DFT calculations the hybrid method was applied (B3LYP) with Becke's three-parameter functional[27] and the nonlocal correlation is provided by the LYP expression.[28] The geometries of all the studied compounds were fully optimized using analytical gradient techniques at both levels. A frequency calculation after each geometry optimization ensured that the calculated structures are real minima or transition states in the potential energy surface of the molecules. For the calculations with

† Electronic supplementary information (ESI) available: optimized bond lengths and angles. See http://www.rsc.org/suppdata/nj/b3/b301191g/

 DOI: 10.1039/b301191g

E = C, Si and Ge, the Gaussian-type basis set 6-311G++(d,p) was employed. In order to have comparable results for all the series with E = C, Si, Ge and Sn, all cage were reoptimized at both levels with the 3-21G++(d,p) basis set. The total energies and zero point energies calculated at various levels and basis sets are given in Table S1.† There were no significant discrepancies of the results obtained with the two basis sets. Thus, the mean deviations of bonds lengths and angles calculated at both levels with the two basis sets are 0.006 Å and 0.2° respectively for the $P_2(HB)_3$, 0.004 Å and 0.1° for $P_2(H_2NB)_3$, 0.009 Å and 0.5° for the $P_2(HB)_2EH_2$ and 0.013 Å and 0.9° respectively for the $P_2(H_2NB)_2EH_2$. Therefore, unless otherwise specified, the discussion is based on the results calculated with the 3-21G++(d,p) basis set. The optimized geometrical parameters calculated using the 6-311G++(d,p) basis set are given in Tables S2, S3 and S4. Although the 3-21G++(d,p) basis set could be considered poor for the description of Sn atom, an optimization at the B3LYP level of $P_2(HB)_2SnH_2$ and $P_2(H_2NB)_2SnH_2$ employing the SDD effective core potential[29] for Sn gave almost identical results shown in Table S5.† The nucleus independent chemical shifts (NICS)[30] were calculated at the MP2 level with both basis sets using the GIAO method.[31] All *ab initio* and DFT calculations were carried out using the GAUSSIAN 98 system of programs.[32]

Results and discussion

An assessment of the computational level and basis sets used in this work, necessary to achieve reasonable comparisons, was made by comparing our results with previous *ab initio* works on $P_2(HB)_3$ and $P_2(H_2NB)_3$, as well as with the available experimental structures for the $P_2(R_2NB)_3$ system. The optimized at B3LYP/3-21G++(d,p) level structures along with selected geometrical parameters are given in Fig. 1. Both molecules adopt the D_{3h} symmetry revealing a trigonal bipyramidal P_2B_3 core analogous to the experimental structures for $P_2(^iPr_2NB)_3$,[33] $P_2(^iPr_2NB)_2((Me_3Si)_2NB)$[34] and $P_2(tmpB)_3$[34] (tmp = 2,2,6,6-tetramethylpiperidino). The calculated equilibrium geometry of $P_2(H_2NB)_3$ compares well with the experimental data. The B–P distance is calculated to be very close to the experimental value (1.952 Å (calc.), 1.95 Å (mean exp)). The calculated B–N distance (1.409 Å) is very close to the experimental distance (mean 1.40 Å). The B···B distance is also well reproduced by the calculations (2.147 Å (calc.), 2.19 Å (mean exp)), as well as the bond angles in the cage. There is an overall agreement of the geometries of the species calculated in this work with those found at the MP2/6-311G(d,p)[25] and MP2/6-31G+(d)[26] levels. Although the perpendicular to the basal plane orientation of the NR_2 units is clearly attributed to steric hindrance in the experimental molecules, the calculations showed that there is also a strong preference for this structure and in the case of the model molecule $P_2(H_2NB)_3$, where no steric hindrance exists. An optimization of the structure with the NR_2 units lying within the basal plane under no symmetry constraint gives also the perpendicular arrangement. This conformational preference is attributed to the higher stabilization of the N lone pairs and the strengthening of the π B–N bond when the NH_2 units lie perpendicular to the basal plane.[25] The introduction of the NH_2 substituent leads to a significant lengthening of the B···B equatorial distance (1.894 to 2.144 Å) and a shortening of the P···P distance (3.134 to 3.015 Å).

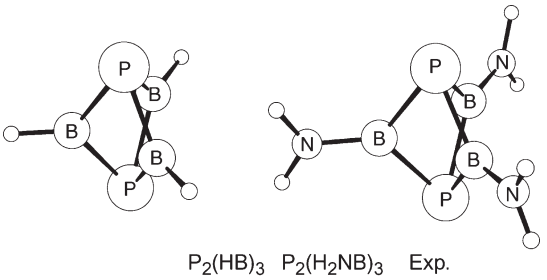

	$P_2(HB)_3$	$P_2(H_2NB)_3$	Exp.
B...B	1.906	2.147	2.190
B-P	1.915	1.952	1.952
B-N		1.409	1.400
B-P-B	59.7	66.7	69.6
P-B-P	109.8	101.2	97.5
B-B-N		129.4	131.2

Fig. 1 Optimized structures and selected geometrical parameters for $P_2(HB)_3$ and $P_2(H_2NB)_3$ at the B3LYP/3-21G++(d,p) level (mean experimental values for $P_2(^iPr_2NB)_2((Me_3Si)_2NB)$ and $P_2(tmpB)_3$).[34]

The geometries of the cage molecules $P_2(HB)_2EH_2$ and $P_2(H_2NB)_2EH_2$ (E = C, Si, Ge) were optimized under the C_{2v} symmetry constraint employing the 6-311G++(d,p) and 3-21G++(d,p) basis set at both MP2 and DFT level of theory. The obtained optimized values of the geometrical parameters using the 3-21G++(d,p) basis set are collected in Tables 1 and 2, whereas their geometries are shown in Fig. 2 and 3. Frequency calculations revealed that all structures are real minima in the potential energy surface, except the case of the $P_2(HB)_2CH_2$ cage, where the C_{2v} structure is a transition state with one imaginary frequency and will be discussed later.

The molecules display a distorted trigonal bipyramidal structure with the two phosphorus atoms occupying the apical position, the HB or NB groups residing in the trigonal basal plane and the H_2N groups lying perpendicular to it. As a result, these P_2B_2E cores resemble the P_2B_3 trigonal bipyramidal core structure of $P_2(R_2NB)_3$.[33,34] A general agreement is found between the calculated and experimental geometries given also for comparison in Table 2. Generally, the largest discrepancies concern the equilibrium bond lengths, while the valence angles are well reproduced at both levels of theory. It is worth noting that the geometrical parameters calculated at the DFT level compare more favorably to experiment than those obtained at the MP2 level.

The C_{2v} optimized structure for the $P_2(HB)_2CH_2$ cage is calculated to be a transition state. Schleyer *et al.*[26] have found also a C_{2v} structure in studying the homodesmotic reaction $P_2(CH_2)_3 + P_2(HB)_2CH_2 \rightarrow P_2(HB)_3 + P_2(HB)(CH_2)_2$. We have repeated their optimization (MP2/6-31G+(d)) and found that it is also a transition state. After releasing the symmetry constraint and reoptimization of $P_2(HB)_2CH_2$ we have located a distorted minimum of C_s symmetry shown in Fig. 2. Its optimized structural parameters are given in Table 1. The basal triangle in this structure is strongly distorted with the carbon atom approaching the first boron atom at a distance only 10% greater that the sum of the boron and carbon atoms covalent radii. This B···B distance is very close to this calculated for $P_2(HB)_3$, for which Schleyer *et al.*[26] predict the delocalized non classical bonding description **1b**. The plot of the relative energy along the intrinsic reaction coordinate (IRC) calculated with this C_{2v} transition state is shown in Fig. 4. From the IRC it is assured that the C_{2v} structure is the transition state in the maximum of the potential energy path (0 $amu^{-1/2}$ bohr) connecting two equivalent C_s structures (−5 and 5 $amu^{-1/2}$ bohr). The barrier height is 12.5 kcal mol^{-1} at the B3LYP/3-21G++(d,p) level and increases to 15.0 kcal mol^{-1} at the MP2 level. This distortion, not found for E = Si, Ge and Sn, should be attributed to strain and/or electronic factors occurring only in the carbon cage. In the C_{2v} structure the C–B–B angles (63.5°) are very close to 60°. This would be energetically penalizing and the C_{2v} structure is unstable. A lesser strain is expected for the cages with E = Si, Ge and Sn, as the E–B–B angles are larger (65°, 66° and 68° respectively). Furthermore, the distorted structure seems to favor the stabilizing interactions between the p orbitals of the carbon and boron

Table 1 Optimized at the MP2 and B3LYP levels bond lengths (Å) and angles (°) for $P_2(HB)_2EH_2$, (E = C, Si, Ge, Sn) using the 3-21G++(d,p) basis set

	$P_2(HB)_2CH_2$ (C_{2v})		$P_2(HB)_2CH_2$ (C_s)[a]		$P_2(HB)_2SiH_2$ (C_{2v})		$P_2(HB)_2GeH_2$ (C_{2v})		$P_2(HB)_2SnH_2$ (C_{2v})	
	MP2	B3LYP	MP2	B3LYP	MP2	B3LYP	MP2	B3LYP	MP2	B3LYP
B···B	1.990	2.046	1.908	1.941	1.957	2.007	1.962	2.011	1.986	2.026
B–P	1.924	1.933	1.909	1.912	1.925	1.933	1.934	1.941	1.937	1.944
			1.899	1.901						
E···B	2.247	2.298	1.737	1.756	2.315	2.362	2.414	2.467	2.605	2.655
			2.439	2.461						
E–P	1.942	1.946	1.987	1.995	2.253	2.261	2.343	2.353	2.554	2.559
B–H	1.193	1.194	1.187	1.189	1.192	1.194	1.193	1.194	1.194	1.195
			1.193	1.194						
E–H	1.092	1.094	1.092	1.095	1.479	1.491	1.525	1.536	1.729	1.741
			1.090	1.090						
B–P–B	62.3	63.9	60.1	61.2	61.1	62.6	61.0	62.4	60.7	62.1
E–P–B	71.1	72.7	52.9	53.4	66.8	68.0	68.0	69.4	69.3	70.7
			77.7	78.3						
P–B–P	99.5	97.4	103.6	102.9	110.6	108.7	111.0	109.0	112.9	110.8
			104.4	103.7						
P–E–P	98.3	96.5	98.0	97.1	89.2	88.0	85.7	84.4	78.4	77.4
B–E–B	52.6	52.8	51.1	51.6	50.0	50.3	47.9	48.1	44.1	44.4
P–B–H	130.2	131.3	127.3	127.7	124.4	125.4	124.1	125.1	122.6	123.8
			126.9	127.1						
B–B–H	143.8	143.3	156.1	156.2	145.8	146.1	144.8	144.9	143.0	143.6
			132.4	132.3						
H–E–H	110.8	110.6	112.3	111.3	107.2	107.5	111.1	111.3	111.1	111.0
α[b]	106.4	105.6	108.9	110.3	126.5	125.5	127.1	126.3	132.0	130.7

[a] The second value for some geometrical parameters refers to B′ (see Fig. 2). [b] α is the angle between the two PEP planes.

atoms. The two occupied molecular orbitals resulting from the interaction of the in plane and the perpendicular to the basal plane carbon and boron orbitals, NHOMO and HOMO respectively, are shown in Fig. 5 for both structures (B3LYP/3-21G++(d,p)). The overlap between the contracted p orbitals of carbon and those of the two boron atoms is small in the C_{2v} structure. In the distorted structure this overlap is higher concerning C–B and B–B′ interactions and lower for the C–B′ interaction. The net result is the stabilization of NHOMO and HOMO in going from the C_{2v} to C_s structure. It should be noted that test optimizations have shown that the hypothetical trigonal $[(HB)_2CH_2]$ fragment adopts also a distorted C_s structure, with the C_{2v} structure being a transition state, a fact that ensures that the distortion is due to the orbital interactions within the basal triangle. No C_s structure has been located also in the case of the $P_2(H_2NB)_2CH_2$ cage, where the interaction of the nitrogen lone pairs with the boron B-p_π orbitals in the equatorial plane of the cage offers a further stabilization. On the other hand, Si, Ge and Sn atoms, which are larger in size and possess more diffuse orbitals, optimize their interaction with boron effectively leading to the stabilization of the symmetrical C_{2v} structure (the r_p orbital radii is

Table 2 Experimental and optimized at the MP2 and B3LYP levels bond lengths (Å) and angles (°) for $P_2(H_2NB)_2EH_2$, (E = C, Si, Ge, Sn) using the 3-21G++(d,p) basis set

	$P_2(H_2NB)_2CH_2$ (C_{2v})		$P_2(H_2NB)_2SiH_2$ (C_{2v})			$P_2(H_2NB)_2GeH_2$ (C_{2v})			$P_2(H_2NB)_2SnH_2$ (C_{2v})		
	MP2	B3LYP	MP2	B3LYP	Exp[a]	MP2	B3LYP	Exp[b]	MP2	B3LYP	Exp[c]
B···B	2.112	2.191	2.125	2.199	2.21	2.126	2.195	2.22	2.134	2.208	2.23
B–P	1.946	1.957	1.951	1.964	1.98	1.955	1.966	1.97	1.960	1.972	1.98
E···B	2.335	2.376	2.403	2.456	2.52	2.489	2.542	2.62	2.676	2.727	2.82
E–P	1.921	1.928	2.248	2.261	2.24	2.337	2.350	2.32	2.549	2.561	2.53
B–N	1.405	1.401	1.410	1.405	1.38	1.409	1.405	1.42	1.411	1.407	1.40
E–H	1.094	1.096	1.482	1.493		1.529	1.541		1.734	1.746	
N–H	1.010	1.014	1.010	1.014		1.010	1.014		1.010	1.014	
B–P–B	65.7	68.1	66.0	68.1	68.7	65.9	67.9	70.0	66.0	68.1	69.1
E–P–B	74.3	75.4	69.4	70.7	73.0	70.2	71.5	74.6	71.5	72.7	76.4
P–B–P	94.3	92.4	105.1	102.9	100.0	105.8	103.6	99.4	107.5	105.1	100.9
P–E–P	95.9	94.2	87.1	85.6	85.2	83.7	82.2	80.7	76.6	75.4	74.2
B–E–B	53.8	54.9	52.5	53.2	52.7	50.6	51.2	51.2	47.0	47.8	46.9
P–B–N	132.8	133.8	127.4	128.5	129.8	127.0	128.1	130.1	126.0	127.2	129.4
B–B–N	144.0	144.9	151.3	152.1	151.3	150.6	151.0	152.4	150.6	151.5	152.9
H–E–H	109.7	109.7	108.1	108.1		110.7	110.6		110.3	109.9	
H–N–H	114.6	114.0	114.6	114.1		114.7	114.2		114.7	114.2	
α[d]	105.9	112.0	127.3	128.0	122.7	128.8	129.1	124.9	133.9	134.1	125.8

[a] Mean values for $P_2(^iPr_2NB)_2(SiPh_2)$ and $P_2(tmpB)_2(SiPh_2)$ (ref. 11). [b] Mean values for $P_2(tmpB)_2(GePh_2)$ (ref. 12). [c] Mean values for $P_2(tmpB)_2(Sn^tBu_2)$ and $P_2(^iPr_2NB)_2(Sn^tBu_2)$ (ref. 13). [d] α is the angle between the two PEP planes.

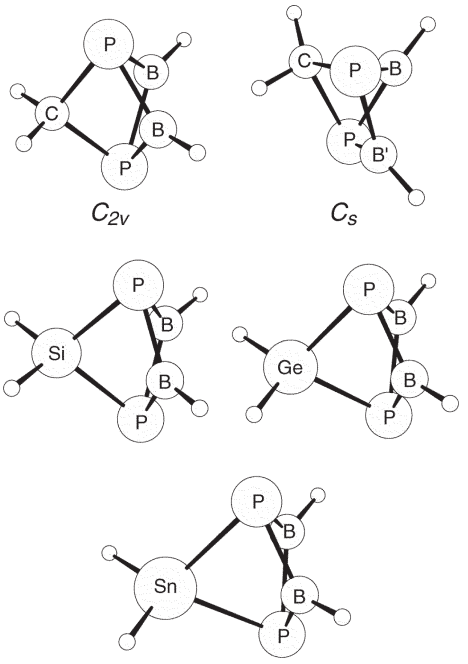

Fig. 2 Optimized structures of $P_2(HB)_2EH_2$, (E = C, Si, Ge and Sn) at the B3LYP/3-21G++(d,p) level.

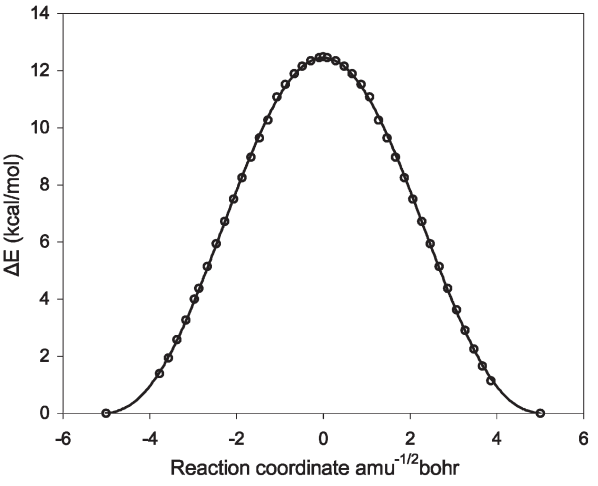

Fig. 4 Plot of the relative energy along the intrinsic reaction coordinate (IRC) calculated at the B3LYP/3-21G++(d,p) level for the C_{2v} transition state of $P_2(HB)_2CH_2$.

0.78, 0.84 and 1.00 au for Si, Ge and Sn respectively compared to 0.25 au for C).[35] Thus, no C_s structure is obtained both for the $P_2(HB)_2EH_2$ cages and for the $[(HB)_2EH_2]$ fragments in this case.

The P–E distances calculated are similar to those in the cage species $(Me_2Si)_6P_4$,[36] $(Me_2Ge)_6P_4$[37] and $(Me_2Sn)_6P_4$[38] (2.244 Å, 2.308 Å, and 2.510 Å respectively). In general there is an almost linear dependence of key geometrical parameters of the cage upon the size and the orbital diffuseness of the element E. Plots of B–B and P···P distances, as well as the P–E–P and the angle α between the two PEP planes, calculated at the B3LYP/3-21G++(d,p) level, *versus* the covalent radii of atom E[39] are given in Fig. 6 and 7 respectively. As the size of E increases the B–B and P···P distances and the angle α increase, whereas the angle P–E–P decreases. From the plots it can be also seen that the values of the structural parameters for the C_s structure of $P_2(HB)_2CH_2$ are quite in line with the other E, while those of the C_{2v} structure are not, particularly in the case of the B···B and P···P distances. The replacement of BH with BNH_2 increases the B···B distances, which lie in the range 1.941 Å–2.046 Å for and 2.191 Å–2.208 Å for $P_2(HB)_2EH_2$ and $P_2(H_2NB)_2EH_2$ respectively.

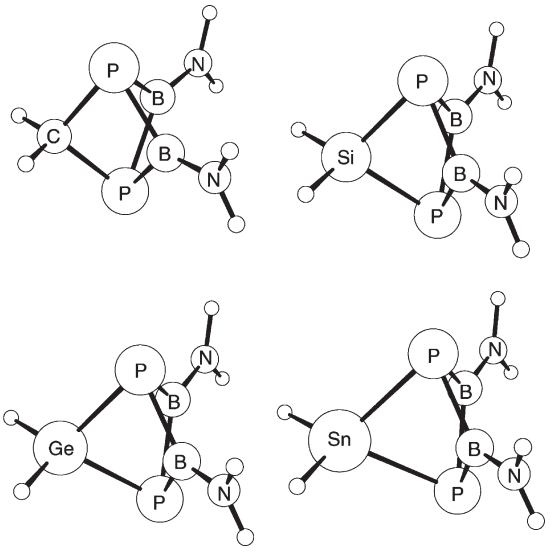

Fig. 3 Optimized structures of $P_2(H_2NB)_2EH_2$, (E = C, Si, Ge and Sn) at the B3LYP/3-21G++(d,p) level.

The nature of bonding in the studied molecules has been characterized by employing the natural population analysis (NPA) of Weinhold, Reed, and Weinstock.[40] The results at the B3LYP/3-21G++(d,p) level are shown in Table 3. The B···B Wiberg bond indices (WBI) and the overlap weighted natural atomic orbitals (NAO) bond orders for $P_2(HB)_2EH_2$ (E = C: C_{2v} structure, Si, Ge, Sn) are smaller than those for $P_2(HB)_3$, for which Schleyer *et al.*[26] predict a boron–boron bonding interaction. NBO bonding descriptions show small deviations from idealized localized Lewis structure, with as much as 94–95% of the total electron density used in describing the Lewis structure (91.6% for $P_2(HB)_3$). The residual electrons (RE), not involved in the two-center bonding and hence delocalized, are in the range 1.15–1.17 *e* (1.78 for $P_2(HB)_3$) and found to be almost independent to basis set and level of calculation. Thus, for $P_2(HB)_3$ the RE are equal to 1.784 and 1.839 *e* for 3-21G++(d,p) and 6-311G++(d,p) respectively at the B3LYP level. The corresponding values at the MP2 level are 1.901 and 1.933 *e*, whereas this calculated by Schleyer *et al.*[26] at the MP2/6-31G + (d) level is 1.823 *e*. The NBO occupancies indicate that each of the boron p_π orbital in the equatorial plane is essentially unoccupied (0.36–0.40 *e*) and favor a localized description for the molecules. This is also supported by the small values of B–E bond indices. The B–P bond indices are close to that of normal B–P single bonds. In the case of the C_{2v} unstable structure of the carbon cage the B–E bond indices are the smallest across the series of $P_2(HB)_2EH_2$. In the distorted C_s structure, which is the minimum, the relatively large B–C bond index confirms the already discussed better overlap between B and C orbitals. Furthermore, a boron–boron interaction is depicted, as all indices are very close to those for $P_2(HB)_3$. The replacement of the BH hydrogens by the NH_2 groups leads to a totally localized description for the $P_2(H_2NB)_2EH_2$ cages (VL ≈ 97%, RE ≈ 0.84 e). In this case, the boron B–p_π orbitals in the equatorial plane of the cage interact with the nitrogen lone pairs and are not available for boron–boron interactions. Thus, the values of B–E bond indices are smaller than those in the corresponding $P_2(HB)_2EH_2$ cages.

Finally, in order to further study the cage delocalization we have also used the nuclear independent chemical shifts (NICSs),[30] defined as the negative of the absolute magnetic

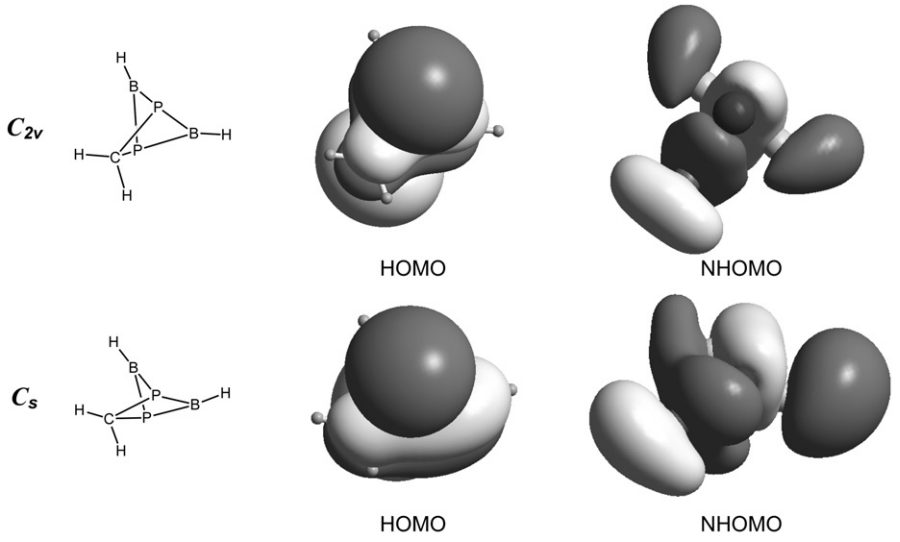

Fig. 5 NHOMO and HOMO molecular orbitals for the C_{2v} and C_s structures of $P_2(HB)_2CH_2$ calculated at the B3LYP/3-21G++(d,p) level.

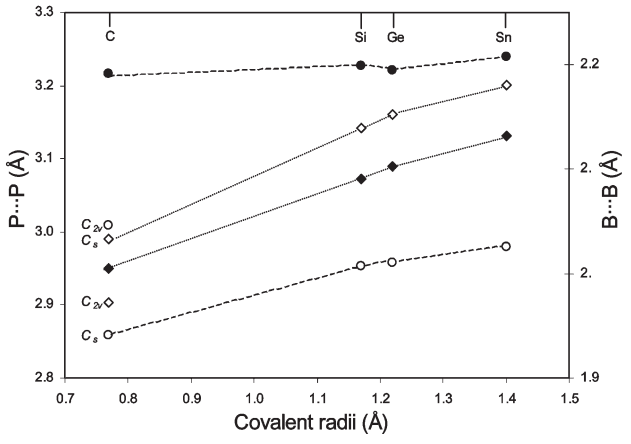

Fig. 6 Plot of the B···B and P···P distances (dashed and dotted lines respectively) calculated at the B3LYP/3-21G++(d,p) level for $P_2(HB)_2EH_2$ (○, ◇) and $P_2(H_2NB)_2EH_2$ (●, ◆) *versus* the covalent radii of atom E = C, Si, Ge and Sn.

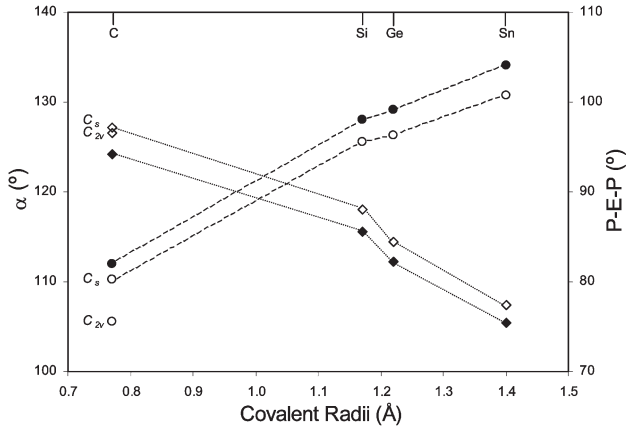

Fig. 7 Plot of the P–E–P and α angles (dotted and dashed lines respectively) calculated at the B3LYP/3-21G++(d,p) level for $P_2(HB)_2EH_2$ (◇, ○) and $P_2(H_2NB)_2EH_2$ (◆, ●) *versus* the covalent radii of atom E = C, Si, Ge and Sn.

shieldings computed at cage centers (nonweighted mean of the heavy atom coordinates). At this position negative NICS values imply delocalization and diatropic current, while positive NICS values paratropic current. NICSs calculated at the MP2 level have been extensively used for the study of two or three-dimensional aromaticity and relative stability of ring heterocycles[30,41] or *closo*-heteroboranes molecular.[26] The calculated NICS values for the cages studied, calculated at the MP2 level with both basis sets, are shown in Table 3. The values for the parent $P_2(HB)_3$ cage are very close to that calculated by Schleyer *et al.*[26] (−18.2 ppm). The very small diatropic NICS of all other molecules, compared to those for $P_2(HB)_3$ and the $B_5H^-_5$ five-vertex deltahedron (–28.1 ppm),[26] show a very limited delocalization, in line with the results of the NPA analysis. The NICS for the unstable C_{2v} transition state of $P_2(HB)_2CH_2$ and for $P_2(H_2NB)_2CH_2$ are paratropic indicating the already discussed absence of any delocalization in the basal plane in the case of the carbon symmetrical cage. The NICS values calculated for the C_s minimum of $P_2(HB)_2CH_2$, where both B–B and C–B interaction in the basal plane exists, are the most diatropic across the series of $P_2(HB)_2EH_2$.

Summary

Ab initio and density functional calculations on a series of five vertex cage compounds of the type $P_2(YB)_2EH_2$, (E = C, Si, Ge, Sn, Y = H, H_2N) using both 6-311G++(d,p) and 3-21G++(d,p) basis sets, indicate that they adopt a trigonal bipyramidal structure of C_{2v} symmetry with the two phosphorus atoms occupying the apical position, the HB or NB groups residing in the trigonal basal plane. The theoretical results agree well with the experimental data for E = Si, Ge and Sn. For the carbon cage $P_2(HB)_2CH_2$ the C_{2v} structure is a transition state and the minimum is a cage of C_s symmetry with a distorted B–B–C ring in the equatorial plane, in which the contacted orbitals optimize their overlap with B and P orbitals leading to both B–B and C–B interaction. Key structural parameters within the cages show a linear dependence on the covalent radii of the heteroatom E. The results of the natural population analysis (NPA) and the values of nucleus independent chemical shifts (NICS) calculated reveal a bonding description very close to an idealized localized Lewis structure for all $P_2(HB)_2EH_2$ cages. When NH_2 groups replace BH hydrogens the classical localized structure is further stabilized.

Table 3 Wiberg bond indices (WBI), natural atomic orbital bond orders (NAO), valence Lewis (VL-in%), B-p_π occupancies, residual electrons (RE) obtained from the natural bond orbital (NBO) analysis[a] and nucleus independent chemical shifts (NICS, ppm) of $P_2(HB)_3$, $P_2(H_2NB)_3$, $P_2(HB)_2EH_2$ and $P_2(H_2NB)_2EH_2$ (E = C, Si, Ge, Sn,) molecules

	WBI			NAO						NICS[b]	
	B–B	B–P	B–E	B–B	B–P	B–E	VL	RE	B-p_π	BS1	BS2
$P_2(BH)_3$	0.436	0.939		0.514	0.819	91.6	1.784	0.504	−16.9	−16.1	
$P_2(BH)_2CH_2(C_{2v})$	0.370	0.923	0.168	0.441	0.819	0.200	94.1	1.151	0.362	2.7	2.9
$P_2(BH)_2CH_2(C_s)$[c]	0.431	0.779	0.534	0.553	0.740	0.660	92.4	1.542	0.457	−13.0	−13.1
		1.039	0.046		0.875	0.000			0.541		
$P_2(BH)_2SiH_2$	0.351	1.038	0.215	0.435	0.873	0.274	94.9	1.133	0.390	−3.3	−3.5
$P_2(BH)_2GeH_2$	0.346	1.043	0.201	0.468	0.883	0.245	95.1	1.104	0.383	−1.8	−2.4
$P_2(BH)_2SnH_2$	0.347	1.066	0.186	0.453	0.883	0.217	94.9	1.167	0.405	—	−2.8
$P_2(BNH_2)_3$	0.239	0.948		0.359	0.827		96.9	1.089	—	−4.9	−4.9
$P_2(BNH_2)_2CH_2$	0.235	0.900	0.086	0.387	0.862	0.158	96.0	1.015	—	0.9	0.4
$P_2(BNH_2)_2SiH_2$	0.216	1.002	0.142	0.340	0.867	0.223	97.3	0.832	—	−2.9	−3.4
$P_2(BNH_2)_2GeH_2$	0.214	1.008	0.133	0.345	0.868	0.186	97.4	0.830	—	−3.2	−3.4
$P_2(BNH_2)_2SnH_2$	0.211	1.024	0.124	0.350	0.874	0.174	97.3	0.874	—	—	−3.7

[a] B3LYP/3-21G++(d,p). [b] Calculated at the MP2 level using the BS1: 6-311G++(d,p) or BS2: 3-21G++(d,p) basis set. [c] The second value for some geometrical parameters refers to B′ (see Fig. 1).

References

1 R. A. Beaudet, in *Advances in Boron and the Boranes*, eds. J. F. Lieman, A. Greenberg and R. E. Williams, VCH, New York, 1988.
2 T. Onak, in *Comprehensive Organometallic Chemistry*, eds. G. Wilkinson, F. G. A. Stone and E. Abel, Pergamon Press, New York, 1982.
3 R. W. Rudolph, *Acc. Chem. Res.*, 1976, **9**, 446.
4 D. M. P. Mingos, *Acc. Chem. Res.*, 1984, **4**, 311.
5 R. N. Crimes, *Carboranes*, Academic Press, New York, 1970.
6 H. Beall, in *Boron Hydride Chemistry*, ed. E. L. Muetterties, Academic Press, New York, 1975, ch. 9; T. Onak, in *Boron Hydride Chemistry*, ed. E. L. Muetterties, Academic Press, New York, 1975, ch. 10; G. B. Dunks and M. F. Hawthorne, in *Boron Hydride Chemistry*, ed. E. L. Muetterties, Academic Press, New York, 1975, ch. 11.
7 K. P. Callahan and M. F. Hawthorne, *Adv. Organomet. Chem.*, 1976, **14**, 145.
8 R. N. Grimes, *Pure Appl. Chem.*, 1974, **39**, 455; K. P. Callahan and M. F. Hawthorne, *Pure Appl. Chem.*, 1974, **39**, 475.
9 D. B. Sowerby, in *The Chemistry of Inorganic Homo- and Heterocycles*, eds. L. Haiduc and D. B. Sowerby, Academic Press, New York, 1987.
10 P. Kölle, G. Linti and H. Nöth, *J. Organomet. Chem.*, 1988, **7**, 355.
11 D. Dou, B. Kaufmann, E. N. Duesler, T. Chen, R. T. Paine and H. Nöth, *Inorg. Chem.*, 1993, **32**, 3056.
12 T. Chen, E. N. Duesler, R. T. Paine and H. Nöth, *Inorg. Chem.*, 1997, **36**, 802.
13 T. Chen, E. N. Duesler, R. T. Paine and H. Nöth, *Inorg. Chem.*, 1997, **36**, 1070.
14 K. Wade, *J. Chem. Soc., Chem. Commun.*, 1971, 792.
15 K. Wade, *Adv. Inorg. Radiochem.*, 1976, **18**, 1.
16 D. A. Dixon, D. A. Klier, T. A. Halgreen, J. H. Hall and W. N. Lipscomb, *J. Am. Chem. Soc.*, 1980, **102**, 2939.
17 R. B. King and D. H. Rouvray, *J. Am. Chem. Soc.*, 1977, **99**, 7834.
18 J. Aihara, *J. Am. Chem. Soc.*, 1978, **100**, 3339.
19 E. D. Jemmis, *J. Am. Chem. Soc.*, 1982, **104**, 7071.
20 R. F. W. Bader and D. A. Legare, *Can. J. Chem.*, 1992, **70**, 657.
21 E. D. Jemmis, G. Subramanian, I. H. Srivastava and S. R. Gadre, *J. Phys. Chem.*, 1994, **98**, 6445.
22 K. Takano, M. Izumo and H. Hosoya, *J. Phys. Chem.*, 1992, **96**, 6962.
23 E. D. Jemmis and G. Subramanian, *J. Phys. Chem.*, 1994, **98**, 9222.
24 R. E. Williams, in *Advances in Organometallic Chemistry*, eds. F. G. A. Stone and R. West, Academic Press, New York, 1994.
25 J. K. Burdett and O. Eisenstein, *J. Am. Chem. Soc.*, 1995, **117**, 939.
26 P. v. R. Schleyer, G. Subramanian and A. Dransfeld, *J. Am. Chem. Soc.*, 1996, **118**, 9988.
27 A. D. Becke, *J. Chem. Phys.*, 1993, **98**, 5648.
28 C. Lee, W. Yang and R. G. Parr, *Phys. Rev. B*, 1988, **37**, 785.
29 (*a*) W. Kuechle, M. Dolg, H. Stoll and H. Preuss, *Mol. Phys.*, 1991, **74**, 1245; (*b*) A. Bergner, M. Dolg, W. Kuechle, H. Stoll and H. Preuss, *Mol. Phys.*, 1993, **80**, 1431.
30 P. v. R. Schleyer, C. Maerker, A. Dransfeld, H. Jiao and N. J. v. E. Hommes, *J. Am. Chem. Soc.*, 1996, **118**, 6317.
31 K. Wolinski, J. F. Hilton and P. Pulay, *J. Am. Chem. Soc.*, 1990, **112**, 8251.
32 M. J. Frisch, G. W. Trucks, H. B. Schlegel, G. E. Scuseria, M. A. Robb, R. Cheeseman, V. G. Zakrzewski, J. A. Montgomery, R. E. Stratman, J. C. Burant, S. Dapprich, J. M. Millam, A. D. Daniels, K. N. Kudin, M. C. Strain, O. Farkas, J. Tomasi, V. Barone, M. Cossi, R. Cammi, B. Mennucci, C. Pomelli, C. Adamo, S. Clifford, J. Ochterski, G. A. Petersson, P. Y. Ayala, Q. Cui, K. Morokuma, P. Salvador, J. J. Dannenberg, D. K. Malick, A. D. Rabuck, K. Raghavachari, J. B. Foresman, J. Cioslowski, J. V. Ortiz, A. G. Baboul, B. B. Stefanov, G. Liu, A. Liashenko, P. Piskorz, I. Komaromi, R. Gomperts, R. L. Martin, D. J. Fox, T. Keith, M. A. Al-Laham, C. Y. Peng, A. Nanayakkara, M. Challacombe, P. M. W. Gill, B. Johnson, W. Chen, M. W. Wong, J. L. Andres, C. Gonzalez, M. Head-Gordon, E. S. Replogle and J. A. Pople, *Gaussian 98*, Revision A.7, Gaussian Inc., Pittsburgh PA, 1998.
33 G. L. Wood, E. N. Duesler, R. T. Paine and H. Nöth, *Phosphorus, Sulfur Silicon Relat. Elem.*, 1989, **41**, 267.
34 D. Dou, G. L. Wood, E. Duesler, R. T. Paine and H. Nöth, *Inorg. Chem.*, 1992, **31**, 3756.
35 A. Zunger, *Phys. Rev.*, 1980, **B22**, 5839.
36 W. Hönle and H. G. v. Schnering, *Z. Anorg. Allg. Chem.*, 1978, **91**, 442.
37 M. Baudler and H. Suchomel, *Z. Anorg. Allg. Chem.*, 1983, **503**, 7.
38 M. Dräger and B. Mathiasch, *Angew. Chem., Int. Ed. Engl.*, 1981, **20**, 1029.
39 J. E. Huheey, E. H. Keiter and R. L. Keiter, *Inorganic Chemistry Principles of Structure and Reactivity*, 4th edn., Harper Collins College Publishers, New York, 1993.
40 A. E. Reed, R. B. Weinstock and F. Weinhold, *J. Chem. Phys.*, 1985, **83**, 135.
41 G. Subramanian, P. v. R. Schleyer and H. Jiao, *Angew. Chem., Int. Ed. Engl.*, 1996, **35**, 2638.